Chemiresistive hydrogen (H_2) gas sensor based on viral-templated Pd nanowires

Chung Hee Moon[1], Yiran Yan[1], Miluo Zhang[2], Nosang V. Myung[2], and Elaine D. Haberer[1,3]

[1]Materials Science and Engineering Program, University of California, Riverside, CA
[2]Department of Chemical and Environmental Engineering, University of California, Riverside, CA
[3]Department of Electrical Engineering, University of California, Riverside, CA

ABSTRACT

A simple, novel technique for chemiresistive H_2 gas sensor fabrication has been developed using an M13 bacteriophage template. The biological template was used to assemble chains of gold (Au) nanoparticles which were covered with palladium (Pd) using electroless deposition, thus producing Au@Pd core-shell nanowires. Sensors were composed of a randomly dispersed, nanowire network and had measured resistances between 1 and 1000 kΩ. Room temperature sensing analysis was completed for H_2 gas concentrations from 100 ppm to 2000 ppm. Device resistance increased with H_2 gas exposure. For these viral-templated Pd nanowire sensors, a maximum response of 160% was found at 2000 ppm and a lowest limit of detection of 6 ppm was determined.

Keywords: M13 bacteriophage, Au-Pd core-shell, Pd nanowires, hydrogen, gas sensor

1 INTRODUCTION

Hydrogen (H_2) gas is a zero emission fuel and a promising alternative energy for powering future vehicles and generating electricity for residential and commercial locations. It is odorless, colorless, and can be extremely combustible. Above 4% concentration in air, it is readily ignited by a tiny spark, heat, or even sunlight [1]. For safe usage of this promising energy source, sensitive and compact H_2 sensors that can rapidly and selectively detect H_2 gas with low power consumption are needed. The U. S. Department of Energy has established target specifications for safety-related H_2 gas sensors that include the detection of H_2 concentrations from 0.1 to 10% in air [2].

A variety of palladium (Pd) nanostructures have been reported as potential materials for chemiresistive H_2 sensors. Pd can selectively interact with H_2 gas to form palladium hydride (PdH_x), which decreases the resistivity of the device [3, 4]. Because the resistance change is controlled by the diffusion of H_2 gas into Pd, nanostructured materials with large surface-to-volume ratios, which facilitate diffusion, are particularly attractive for rapid sensing response and recovery. Some examples of nanostructures used in H_2 sensors include nanowires, nanotubes, nanoparticle arrays, and thin films [5-8].

Several bio-templated, nanostructured chemiresistive gas sensors have been studied [9-11]. The structurally complex nature of many biological materials allows facile assembly of distinctive inorganic nanostructures that cannot be created using conventional techniques. For example, cotton fibers, bacteria, and eggshells have been used to form In_2O_3 microtubules, ZnO hollow spheres, and SnO_2 fibrous matrices, respectively, for highly sensitive gas detection [11-13]. Yet, for optimum performance, these sensors typically require high temperatures during fabrication and sensor operation, which increases power consumption and costs during manufacturing and use.

Here, we have utilized a filamentous M13 bacteriophage to assemble Pd-based, nanowire chemiresistive gas sensors at room temperature which are able to detect low concentrations of H_2 gas under ambient conditions. The M13 bacteriophage, approximately 880 nm in length and 6 nm in diameter, has a high aspect ratio which is suitable for nanowire assembly [14]. Using the M13 bacteriophage as a template, nanowires have been formed from a number of inorganic materials including gold, ZnS, and $Cu_{1.8}S$ [15-17]. In this work, the role of the viral template was to assist in the organization of one-dimensional chains of Au nanoparticles which were then coated with Pd to form Au@Pd core-shell nanowire-based gas sensors. The preliminary assembly and operation of these chemiresistive gas sensors are described, demonstrating the potential of this approach for H_2 detection. Further studies are required to fully understand this sensor system.

2 EXPERIMENTAL DETAILS

2.1 Viral-templated Sensor Fabrication

A previously reported assembly method was adapted for fabrication of viral-templated, Au@Pd core-shell nanowire gas sensors [18, 19]. Using standard microfabrication techniques, gold electrodes 50 μm wide and 3 μm apart were pre-patterned on Si/SiO_2 substrates and activated with O_2 plasma. Gold-binding M13 bacteriophage [15] were randomly adsorbed onto these pre-patterned substrates through incubation in a solution of phage at a concentration of $3x10^8$ pfu/μL for 10 min. The samples were then washed with tris-buffered saline with 0.7% Tween 20 (TBST), rinsed with deionized water, and incubated in 5 nm gold nanoparticle solution (BBI Solution) for 1 hr for selective decoration of the phage template. Then, the samples were rinsed again with deionized water, and gently air dried. The template-bound gold nanoparticles were enlarged through a

process of electroless deposition using Nanoprobes GoldEnhance™ LM solutions for 1 min. These gold nanostructures were used as seeds for electroless deposition of Pd to form Au@Pd core-shell nanowires. Each substrate with viral-templated gold nanostructures was placed in 1187.5 μL of H_2PdCl_4 (3.79 mM) and 312.5 μL of ascorbic acid (115.2 mM) was slowly added over a span of 30 min while stirring. To increase Pd thickness, the deposition process was repeated and the sample was allowed to incubate an additional 10 minutes. Between deposition steps, the sample was washed with deionized water and gently air dried.

2.2 Morphological and Electrical Characterization

A scanning electron microscope (SEM, 10 kV, Philips XL30) was used to characterize the size, morphology, and areal distribution of the viral-templated Pd nanowires within the device. Two-terminal current-voltage (I-V) measurements were performed to determine the electrical resistance of the devices. For each device, the current was measured while the voltage was swept from -0.3 V to 0.3 V (Keithley 2636A sourcemeter).

2.3 Sensor Performance Analysis

Sensing behavior was evaluated on selected devices which were wire-bonded (West-bond Inc. 7499D) to a copper printed circuit board (PCB) with 1% Si/Al wire prior to sensing. The wire-bonded sensors were placed in a closed Teflon chamber with gas inlet and outlet. The resistance was recorded while applying a constant bias of 0.15 V. The chamber was purged with dry air for 5 hrs to establish a stable baseline resistance, then the sensors were alternately exposed to H_2 gas for 15 min and dry air for 30 min. Following each dry air purge, the concentration of H_2 gas was increased such that sensing analysis was sequentially completed at 100, 200, 250, 500, 1000, 1500, and 2000 ppm. A mass flow controller with LabVIEW interface was used to control the gas concentration and exposure time during sensing analysis.

3 RESULT AND DISCUSSION

3.1 Morphology and Electrical Characteristics of Viral-templated Nanowires

SEM images in figure 1(a)-(c) show areal distribution and morphology of the viral-templated Au@Pd core-shell nanowires within the fabricated devices. Figure 1(a) is a representative image of viral-templated Au@Pd core-shell nanowires bridging the 3 μm gap between electrodes. The nanowires, which were slightly less than 1 μm in length, were arranged in a random network, physically and electrically connecting the two electrodes. Variations in

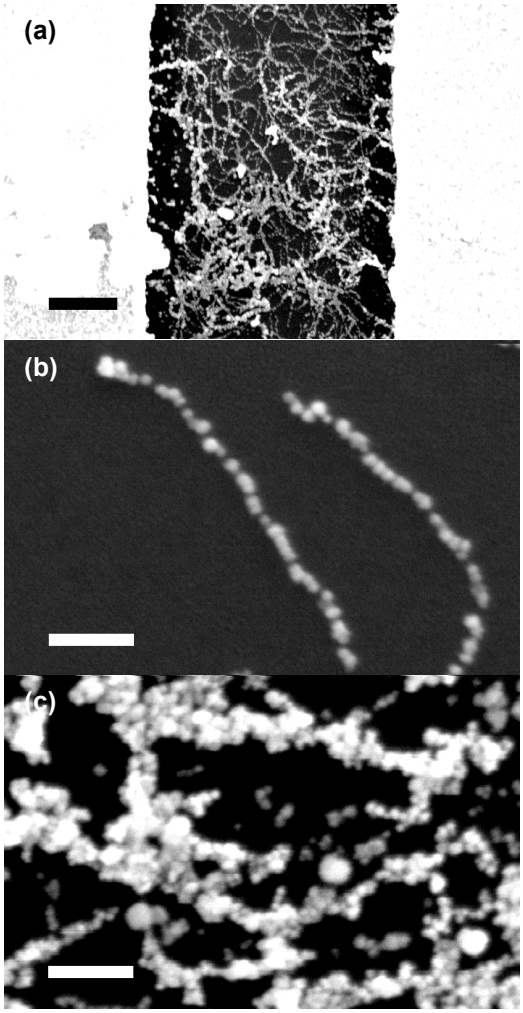

Figure 1. Morphology of viral-templated nanowires within a gas sensor. Scanning electron microscope images of (a) a viral-templated Au@Pd core-shell nanowire device. Scale bar is 1 μm. High magnification images of biologically-templated Au@Pd core-shell nanowires (b) before and (c) after Pd deposition. Scale bars are 200 nm.

width were observed within individual nanowires, as well as from nanowire to nanowire. High magnification SEM images in figure 1(b) and (c) show viral-templated materials before and after Pd deposition, respectively. Before Pd deposition, the enlarged Au nanoparticles were small and isolated. Pt/Pd sputtering was required to prevent charge build-up and allow SEM visualization. Low gold nanoparticle connectivity was apparent along the template length, with large gaps between nanoparticles clearly visible in many locations. As shown in the high-magnification image in figure 1(c), after Pd deposition, continuous nanowires were formed with an average width of 49±15 nm. Nanocrystalline Pd deposition was not conformal, but rather composed of unevenly distributed, irregularly sized clusters. Due to the nonuniform Pd coverage, a range of connectivity was observed within each device such that some nanowires and/or portions of

nanowires were physically disconnected from the nanowire network.

Current-voltage (I-V) measurements were performed on the viral-templated devices before and after Pd deposition by sweeping the voltage from -0.3 V to 0.3 V. Before Pd deposition, no measureable current flow was observed in the devices, which were composed of discontinuous chains of Au nanoparticles. However, after Pd deposition, the devices displayed Ohmic behavior with electrical resistances between 1 and 1000 kΩ. The change in electrical behavior was attributed to the enhanced connectivity created by the Pd deposition. As shown in the SEM images in figure 1(b) and (c), the addition of a Pd shell to the chains of viral-templated Au nanoparticles created continuous Au@Pd core-shell nanowires capable of supporting electrical current.

3.2 Sensing Analysis of Viral-templated Device

Room temperature sensing analysis of the viral-templated devices was performed for H_2 gas concentrations between 100 ppm and 2000 ppm. Representative sensing behavior is shown in figure 2. Sensor resistance increased relative to the baseline resistance when exposed to H_2 gas and partially recovered or returned to near baseline resistance when subsequently exposed to dry air flow. The increase in resistance with exposure to H_2 gas was consistent with reports of single Pd nanowire sensors for H_2 concentrations below 2%, the PdH_x alpha-beta phase transition threshold [5, 20-22]. In this regime, H_2 interacts with Pd forming PdH_x and reducing conductivity. The sensor response, $\Delta R/R_0$ (%), increased with H_2 gas concentration within the evaluated range; no evidence of response saturation was observed. At 2000 ppm H_2, the highest concentration evaluated in these studies, the viral-templated device showed a response of 160%. The response of the viral-templated Au@Pd core-shell nanowire H_2 sensors was comparable to those reported and tested in similar concentration ranges [5, 22-24]. The initial sensor response and recovery were more rapid at higher analyte concentrations, however the overall recovery of these devices decreased with increasing analyte concentration such that 98 % and 71 % recovery was observed at 100 and 2000 ppm, respectively, after 30 minutes. The lowest detection limit, defined as the concentration at which the response is 3 times the baseline signal-to-noise ratio, was calculated to be 6 ppm. These preliminary results confirm the feasibility of using viral-templated Au@Pd core-shell nanowires for H_2 gas detection. Additional studies are currently underway to expand device understanding and improve sensor performance.

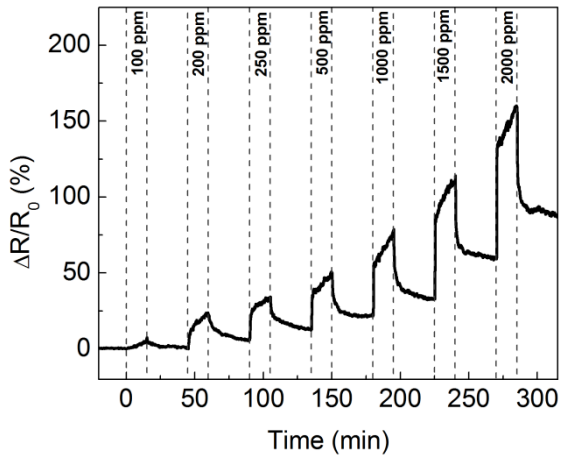

Figure 2. Representative sensing behavior of a viral-templated device to H_2 gas concentrations between 100 ppm and 2000 ppm. The sensor was alternately exposed to H_2 gas and dry air at 15 min and 30 min intervals, respectively.

4 CONCLUSION

Here, we report fabrication of viral-templated Au@Pd core-shell nanowires for sensitive chemiresistive H_2 gas detection under ambient conditions. Pd nanowires were formed from chains of electrically conductive Au@Pd core-shell nanoparticles and incorporated into devices as randomly dispersed networks. This assembly approach produced sensors with a broad electrical resistance distribution ranging from 1 to 1000 kΩ. In addition, the nanowire-based devices showed sensitive response to low concentrations of H_2 from 100 ppm to 2000 ppm, with a maximum response of 160% to 2000 ppm. These are promising initial steps for development and understanding of highly sensitive H_2 gas sensors using a novel viral-templated assembly technique.

ACKNOWLEDGEMENT

The authors thank E. L. Hu (Harvard) and A. M. Belcher (MIT) for the gift of the gold-binding bacteriophage (p8#9). Parts of this study were performed at the Central Facility for Advanced Microscopy and Microanalysis (CFAMM) and the Center for Nanoscale Science and Engineering (CNSE) at UCR.

REFERENCE

[1] Schroder V, Emonts B, Janssen H and Schulze H P 2004 *Chem. Eng. Technol.* **27** 847-51
[2] Butter W, Burgess R, Post M and Rivkin C 2012 (Golden, Colorado: National Renewable Energy Laboratory, U.S. Department of Energy)
[3] Lewis F A 1967 (London: Academic Press)
[4] Hughes R C and Schubert W K 1992 *J. Appl. Phys.* **71** 542-4
[5] Yang F, Kung S-C, Cheng M, Hemminger J C and Penner R M 2010 *Acs Nano* **4** 5233-44
[6] Lim J H, Park J, Ahn J H, Jin H J, Hong S and Park T H 2013 *Biosens. Bioelectron.* **39** 244-9

[7] Xie B, Zhang S, Liu F, Peng X, Song F, Wang G and Han M 2012 *Sens. and Actuators A-Phys* **181** 20-4
[8] Lee J, Shim W, Lee E, Noh J-S and Lee W 2011 *Angew. Chem. Int. Ed.* **50** 5301-5
[9] Peng W, Zhu C, Zhu S, Yao F, Li Y and Zhang D 2013 *J. Mater. Sci.* **48** 4336-44
[10] Liu Z, Fan T, Zhang D, Gong X and Xu J 2009 *Sens. and Actuators B-Chem* **136** 499-509
[11] Song P, Wang Q and Yang Z 2012 *Sens. and Actuators B-Chem* **168** 421-8
[12] Zhang H, Xu C, Sheng P, Chen Y, Yu L and Li Q 2013 *Sens. and Actuators B-Chem* **181** 99-103
[13] Dong Q, Su H, Zhang D and Zhang F 2006 *Nanotechnology* **17** 3968-72
[14] Sidhu S S 2001 *Biomol. Eng.* **18** 57-63
[15] Huang Y, Chiang C Y, Lee S K, Gao Y, Hu E L, De Yoreo J and Belcher A M 2005 *Nano Lett.* **5** 1429-34
[16] Flynn C E, Mao C B, Hayhurst A, Williams J L, Georgiou G, Iverson B and Belcher A M 2003 *J. Mater. Chem.* **13** 2414-21
[17] Zaman M S, Moon C H, Bozhilov K N and Haberer E D 2013 *Nanotechnology* **24** 325602
[18] Haberer E D, Joo J H, Hodelin J F and Hu E L 2009 *Nanotechnology* **20** 4215206
[19] Moon C H, Zhang M, Myung N V and Haberer E D 2013 *Nanotechnology* **25** 135205
[20] Im Y, Lee C, Vasquez R P, Bangar M A, Myung N V, Menke E J, Penner R M and Yun M H 2006 *Small* **2** 356-8
[21] Jeon K J, Lee J M, Lee E and Lee W 2009 *Nanotechnology* **20** 135502
[22] Sennik E, Kilinc N and Ozturk Z Z 2010 *J. Appl. Phys.* **108** 054317
[23] Jeon K J, Jeun M, Lee E, Lee J M, Lee K-I, von Allmen P and Lee W 2008 *Nanotechnology* **19** 495501
[24] Zeng X Q, Latimer M L, Xiao Z L, Panuganti S, Welp U, Kwok W K and Xu T 2011 *Nano Lett.* **11** 262-8